



OPEN Plasma proteomic analysis reveals altered protein abundances in HIV/ HBV co-infection individuals with HCC and with liver cirrhosis

Yongxi Zhang^{1,2,5}, Ping Xu^{1,5}, Xingxia Yu^{3,5}, Ke Zhuang⁴, Xien Gui^{1,2} & Rongrong Yang^{1,2}✉

To develop a risk prediction model for hepatocellular carcinoma (HCC) by screening differentially expressed proteins (DEPs) in HIV/HBV coinfected patients with HCC and liver cirrhosis using proteomic techniques. DEPs were identified in plasma from HIV/HBV co-infected patients with HCC and liver cirrhosis using quantitative liquid chromatography-mass spectrometry (LC-MS). Mapping discovered proteins to the Gene Ontology (GO), Kyoto Encyclopedia of Genes and Genomes (KEGG), and Disease Ontology (DO) databases yielded annotation information for DEPs. Differential plasma apolipoprotein A-1 (APOA1) and transthyretin (TTR) expression levels were validated in 88 HIV/HBV co-infected individuals with HCC and liver cirrhosis. In total, 150 DEPs were discovered. The GO entries were primarily enriched for cutaneous immunological response mediated by circulating immunoglobulin and complement activation, as well as lipoprotein particle. The KEGG pathway enrichment was dominated by complement and coagulation cascades. Six of the 15 items enriched in the DO entries were related to lipid metabolism. APOA1, TTR, Prothrombin (F2), Antithrombin-III (SERPINC1), Alpha-2-HS-glycoprotein (AHSG), Alpha-2-macroglobulin (A2M) and Haptoglobin-related protein (HPR) were finally identified as hub proteins. Finally, a visual logistic model using immunoglobulin heavy variable 3–13 (IGHV3-13) and A2M to predict HCC were constructed. Significant variations in plasma APOA1 and TTR levels were found in HIV/HBV co-infected patients with HCC and liver cirrhosis. The screened hub proteins from DEPs can be employed as possible markers for early HCC detection. The developed HCC prediction model can be used to assess the risk of HCC in HIV/HBV co-infected cirrhotic individuals.

Keywords Liver cirrhosis, Hepatocellular carcinoma, Human immunodeficiency virus, Lipid metabolism, Apolipoprotein A-1, Transthyretin

Abbreviations

A2M	Alpha-2-macroglobulin
AFP	alpha fetoprotein
AHSG	Alpha-2-HS-glycoprotein
APOA1	Apolipoprotein A-I
ART	antiretroviral therapy
AUC	Area Under Curve
BP	Biological process
CAA	2-Cyanoacetamide
CHB	chronic hepatitis B
DCA	Decision curve analysis
DEPs	differentially expressed proteins
DIA	Data Independent Acquisition
DMNC	Density of Maximum Neighborhood Component
DO	Disease Ontology

¹Department of Infectious Diseases, Zhongnan Hospital of Wuhan University, Wuhan, Hubei, China. ²Center for AIDS Research, Wuhan University, Wuhan, Hubei, China. ³Department of Emergency, Renmin Hospital of Wuhan University, Wuhan, Hubei, China. ⁴ABSL-III Laboratory at the Center for Animal Experiment, State Key Laboratory of Virology, Wuhan University, Wuhan, Hubei, China. ⁵Yongxi Zhang, Ping Xu and Xingxia Yu contributed equally to this work. ✉email: yangrr1130@126.com

F2	Prothrombin
FDR	False discovery rate
GO	Gene Ontology
HBV	hepatitis B virus
HCC	hepatocellular carcinoma
HCD	high-energy collisioninduced dissociation
HPR	Haptoglobin-related protein
IGHV3-13	immunoglobulin heavy variable 3–13
KEGG	Kyoto Encyclopedia of Genes and Genomes
LASSO	Least absolute shrinkage and selection operator
LC-MS	liquid chromatography-mass spectrometry
MCC	Maximal Clique Centrality
MNC	Maximum Neighborhood Component
PCA	principal component analysis
PLWH	people living with HIV
PPIs	protein-protein interactions
SDC	Sodium deoxycholate
SERPINC1	Antithrombin-III
TCEP	Tris(2-carboxyethyl) phosphine
TFA	Trifluoroacetic acid
Tris-HCL	Tris(hydroxymethyl) Aminomethane Hydrochloride
TTR	Transthyretin

Hepatocellular carcinoma (HCC) is a major health problem with an increasing frequency worldwide, and it is frequently preceded by chronic liver diseases. Chronic hepatitis B (CHB) infection is one of the most common etiologies of HCC¹. China is a moderately endemic area for hepatitis B virus (HBV), with a positive incidence of HBsAg in the general population of 6.89%² and a positive rate of 10.0% in people living with HIV (PLWH)³. Globally, the prevalence of CHB infection is 8.4% among PLWH, which could be extrapolated to an estimated population of 3 136 500 (95% CI, 2 952 000–3 284 100) cases of HBV in PLWH⁴. As the HIV-infected population has aged during the antiretroviral therapy (ART) era, HCC has emerged as a prominent cause of non-AIDS-defining cancer and cancer-attributable death⁵.

Ultrasound and serum alpha fetoprotein (AFP) detection are commonly used to diagnose HCC, although ultrasound is difficult to identify tumors 3 cm in size and cannot entirely distinguish benign and malignant tumors⁶. Although AFP is a traditional indication of HCC, it can also be elevated in benign liver disorders such as hepatitis and cirrhosis⁷, and negative AFP occurs in 15–30% of advanced HCC⁸. Thus, AFP is no longer recommended by the American Association for the Study of Liver Diseases Practice Guidelines Committee for the early detection of HCC⁹. Although developments in computed tomography and magnetic resonance imaging technology have substantially improved HCC diagnostic performance, these techniques are now too costly for widespread screening. Therefore, it is critical to develop a low-cost, specific serological marker for early detection of HCC.

With the advancement of high-throughput sequencing, gene chips, and mass spectrometry, a growing number of chronic HBV infection-related disorders are utilizing omics-based research to identify new biomarkers at the genomic, transcriptomic, proteomic, and metabolomic levels^{10,11}. Unfortunately, these signs have yet to be widely used in clinical practice. Because peripheral venous blood collection is the most acceptable method of detection for patients, blood is a simple specimen to obtain clinically. Protein concentrations of various serum components are currently the most regularly measured analytes in clinical practice, accounting for 41.9%¹². Proteomic technology has various advantages, including excellent reproducibility, accuracy, sensitivity, specificity, and sample multiplexing. Although a tandem mass tag-based quantitative proteomics technique has shown proteome characterisation of the natural history of chronic HBV infection¹³, little attention has been paid to the use of proteomic technologies for HCC discrimination in HIV/HBV co-infected individuals. Plasma proteomics using mass spectrometry may discover a wide range of disease-related hallmark proteins, which is important for clinical diagnosis, treatment, prognosis, and etiology research. The goal of this work was to employ quantitative liquid chromatography tandem mass spectrometry (LC-MS/MS) to discover differentially expressed proteins (DEPs) in HIV/HBV co-infected persons with HCC and liver cirrhosis, which could aid in early diagnosis of HCC and identification of target molecules for early treatment, which is crucial in cancer therapy.

Methods

Patients

Patients diagnosed with HIV/HBV co-infection at Wuhan University's Zhongnan Hospital between March 1, 2021 and December 31, 2022 were eligible to take part in this study. The following were the inclusion criteria: (1) 30–70 years old; (2) complete HIV clinical information, including ART status and current CD4+ T lymphocyte counts; (3) complete HBV clinical information, including hepatitis B markers, HBV DNA levels, and liver imaging evaluation findings; and (4) had a clear diagnosis of cirrhosis or HCC. The following were listed as exclusion criteria: (1) being pregnant or nursing, (2) having an uncontrolled underlying illness, (3) having organ dysfunction, (4) liver diseases brought on by other hepatitis virus infections, (5) having any malignancy other than HCC, and (6) having diseases other than viral hepatitis that may cause liver cirrhosis, such as metabolic disorders, use of alcohol or drugs, and hereditary conditions.

Proteomic analysis necessitated exact matching of age, gender, and clinical routine test indexes, as well as CD4+T lymphocyte counts, HBeAg status, liver function results, duration of HBV infection, HIV and HBV replication levels, and other known factors influencing HCC and liver cirrhosis progression. Given that all of the prerequisites for proteomic analysis are met, patients living with HIV and HBV coinfection who were successfully matched were separated into HCC and liver cirrhosis groups for future proteome research.

This study was approved by the institutional review board of the Zhongnan Hospital of Wuhan University(2021022). All methods were performed in accordance with the relevant guidelines and regulations. An informed consent form was signed by all patients.

Sample preparation

Blood samples were collected from patients between March 2021 and December 2022. Plasma proteins were digested with trypsin (1:50 w/w) following standard reduction and alkylation procedures. High-abundance proteins were removed using a commercial depletion kit (ProteoExtract™, Merck). Peptides were purified and stored at -20°C for subsequent proteomic analysis.

LC-MS/MS analysis

To increase identification of low-abundance proteins, high-abundance proteins were first depleted from serum samples using LC-MS/MS. Then, trypsin was used to breakdown the proteins, and the resultant peptides were desalted and prepared for analysis.

Peptides were separated on a C18 column using a nanoflow LC system with a gradient of 0.1% formic acid in water (mobile phase A) and 0.1% formic acid in 80% acetonitrile (mobile phase B). The eluted peptides were analyzed using an Orbitrap mass spectrometer operated in data-dependent acquisition (DDA) or data-independent acquisition (DIA) mode. In DDA mode, full-scan MS spectra were acquired followed by MS/MS scans of the most intense ions. In DIA mode, full-scan MS spectra were followed by variable MS/MS scans. High-field asymmetric waveform ion mobility spectrometry (FAIMS) was used to enhance ion separation.

Library search

In brief, the raw MS data were analyzed using DIA-NN software (V1.8.1, <https://github.com/vdemichev/DiaNN>) and referred to the Human proteome database in Uniprot. After extracting the raw DIA data, the protein quantitative information was retrieved by merging the MBR function and the predictive spectrum library in DIA-NN utilizing the deep learning technique. The protein and precursor's ultimate False discovery rate (FDR) was set at 1%. The DIA-NN output files including quantification data for protein groups were used for later analysis.

Biological information analysis

The databases, which primarily include Gene Ontology (www.geneontology.org)(GO), Kyoto Encyclopedia of Genes and Genomes (<http://www.genome.jp/kegg/>)(KEGG), and Disease Ontology (<https://disease-ontology.org/>)(DO), are used to annotate the identified proteins in order to determine the functional properties of DEPs. Furthermore, CytoScape software (Version 3.10.1, <https://cytoscape.org/download.html>) was utilized to create network maps of DEPs with human known protein-protein interactions (PPIs) using the STRING database.

Plasma apolipoprotein A-1 (APOA1) and transthyretin (TTR) measurements

Plasma APOA1 and TTR are routine clinical testing items, and the methods for detection were as reported in References^{14,15}.

Statistical analysis

The early screening of biomarkers was based on multiple of difference (FC) and statistical test ($p < 0.05$). Further LASSO regression was performed to exclude out DEPs that were not directly associated to the condition under study. The discrimination of the model was evaluated using the C-Index, Area Under Curve (AUC), or C-Statistics; the calibration curve was used to analyze the calibration of the clinical prediction model; the clinical effect of the model was assessed using a nomogram or the Decision curve analysis (DCA). Software from IBM SPSS (Version 29, <https://www.ibm.com/products/spss-statistics/trial>) and the R project “glmnet” package (Version 4.1-8, <https://glmnet.stanford.edu/>) were used for statistical analysis and model building methods. All statistical tests were two-tailed, and a value of $p < 0.05$ was regarded as indicating statistical significance.

Results

Patient characteristics

This study included 114 individuals with HIV/HBV co-infection, with 43 patients assigned to the HCC group and the remaining 71 liver cirrhosis patients assigned to the control group. Table 1 summarizes the individuals' demographic and clinical features. Plasma samples from 26 patients who were matched by age, gender, and clinical indicator associated with HIV and HBV infection were included in the proteomic analysis. The workflow for research procedure was shown as Fig. 1.

Differential protein analysis

Twenty-six proteomes were examined using the DIA technique, yielding a total of 653 proteins and 8196 precursors (Fig. 2A and B). Differential abundance analysis revealed that a total of 150 proteins were significantly dysregulated ($|\log_2\text{FC}| \geq 0.58$, $p \leq 0.05$) in the HCC group compared to the liver cirrhosis group, with 93 proteins upregulated and 57 proteins downregulated (Fig. 2C). The principal component analysis (PCA) plot of the intensities of these 150 DEPs demonstrated a distinct separation between HCC and liver cirrhosis (Fig. 2D). The

	People living with HIV/HBV co-infection		Statistics	p	DEPs samples		Statistics	p
	Diagnosed with HCC	Diagnosed with liver cirrhosis			Diagnosed with HCC	Diagnosed with liver cirrhosis		
Cases	43	71	–	–	13	13	–	–
Male (n,%)	41(95.3)	66(93.0)	0.266	0.606	12(92.3)	12(92.3)	–	–
Age, mean \pm SD	52.8 \pm 2.4	50.3 \pm 3.5	0.604	0.547	50.8 \pm 3.2	51.3 \pm 2.8	0.624	0.545
cART treatment (n,%)	22(51.2)	37(52.1)	0.010	0.922	7(53.8)	7(53.8)	–	–
Anti-HBV therapy (n,%)	22(51.2)	37(52.1)	0.010	0.922	7(53.8)	7(53.8)	–	–
CD4 ⁺ T cell count (cells/ μ L)	156 \pm 25	162 \pm 28	0.450	0.654	160 \pm 28	165 \pm 21	0.358	0.685
Log ₁₀ HIV-RNA (mean \pm SD)	4.60 \pm 0.22	4.61 \pm 0.28	0.102	0.919	4.61 \pm 0.25	4.63 \pm 0.18	0.215	0.806
HBeAg (n,%)	8(18.6)	15(21.1)	0.106	0.745	2(15.4)	2(15.4)	–	/
Log ₁₀ HBV-DNA (mean \pm SD)	3.05 \pm 0.44	3.42 \pm 0.30	0.512	0.610	4.05 \pm 0.24	4.12 \pm 0.30	0.114	0.712
Blood routine test (mean \pm SD)								
White blood cells (10^9 /L)	4.20 \pm 0.22	4.02 \pm 0.41	0.320	0.750	4.25 \pm 0.42	4.27 \pm 0.50	0.300	0.765
Hemoglobin (g/L)	112.8 \pm 10.2	122.3 \pm 14.2	0.526	0.600	122.5 \pm 12.3	127.4 \pm 13.2	0.406	0.682
Platelets (10^9 /L)	125.5 \pm 14.2	127.4 \pm 20.3	0.886	0.377	115.0 \pm 18.2	124.7 \pm 23.8	0.902	0.301
Liver function test (mean \pm SD)								
ALT (U/L)	36.6 \pm 4.5	38.5 \pm 2.8	0.896	0.372	37.0 \pm 4.2	39.5 \pm 3.8	0.812	0.352
AST (U/L)	36.5 \pm 4.2	39.2 \pm 6.7	0.850	0.397	38.5 \pm 5.2	39.7 \pm 4.7	0.550	0.697
Tbil (μ mol/L)	10.2 \pm 2.7	10.5 \pm 1.9	0.630	0.530	10.6 \pm 1.7	11.5 \pm 1.2	0.736	0.452
Alb(g/L)	40.2 \pm 5.5	42.4 \pm 4.8	1.036	0.302	41.8 \pm 4.5	44.0 \pm 3.8	1.006	0.321

Table 1. Clinical characteristics of people living with HIV/HBV co-infection and depts samples. SD, standard deviation; cART, Combination antiretroviral therapy; ALT, alanine aminotransferase; AST, aspartate aminotransferase; Tbil, total bilirubin; Alb, albumin.

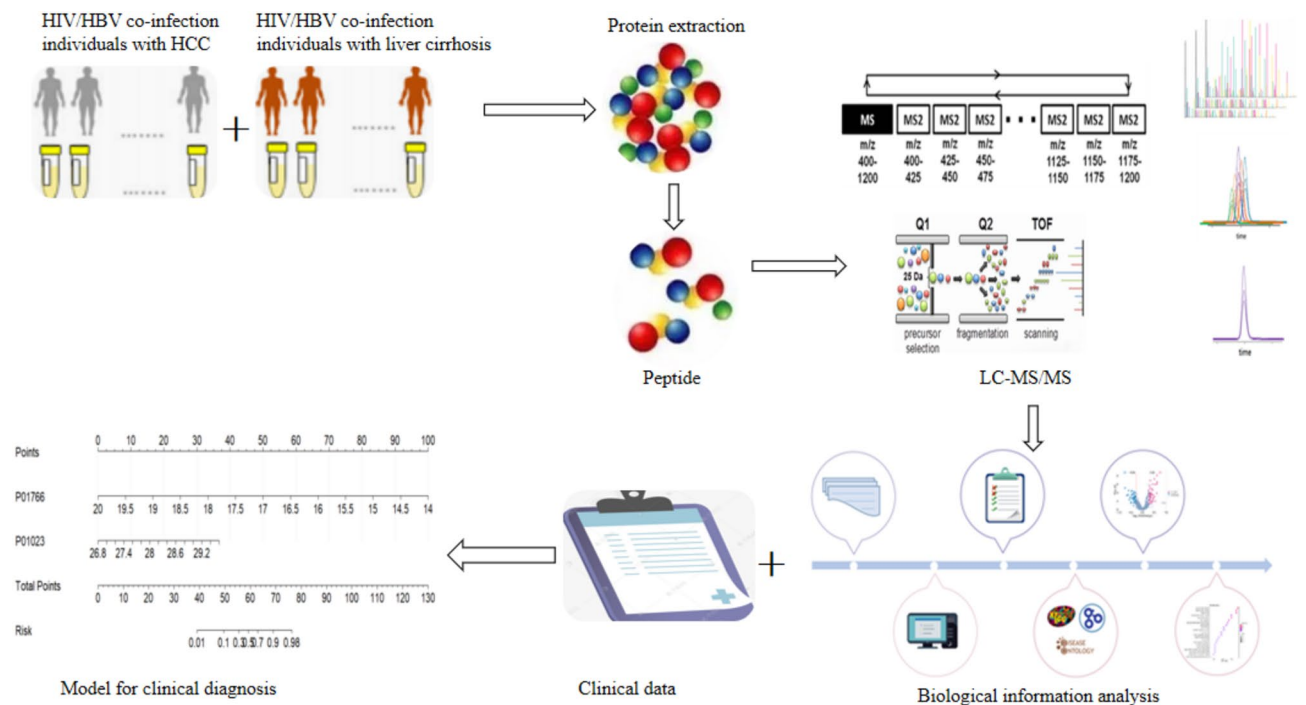


Fig. 1. The workflow for research procedure.

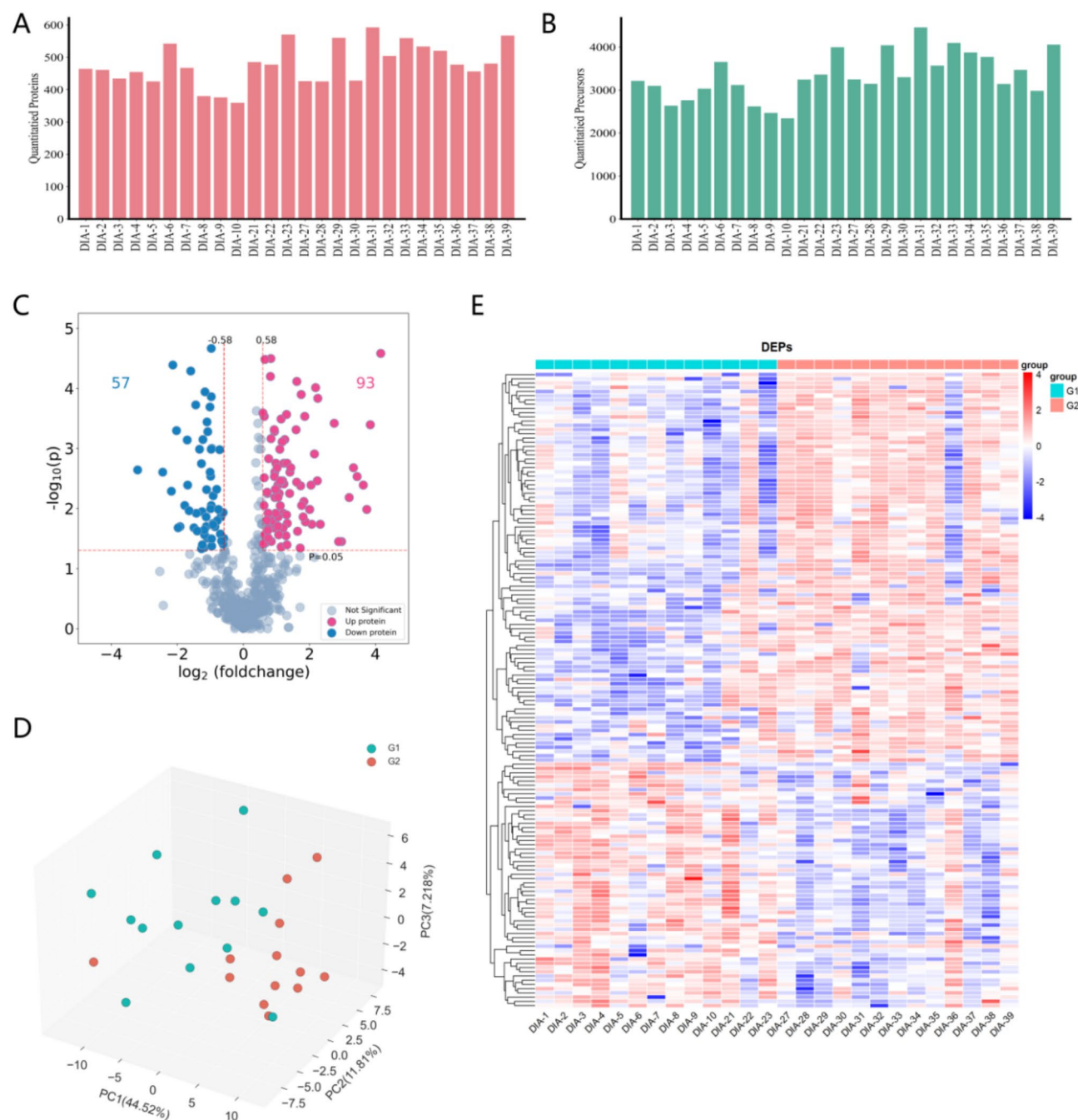


Fig. 2. Differently expressed proteins (DEPs) in patients with HCC and with liver cirrhosis. **(A, B)** The distribution of numbers of quantified **(A)** proteins and **(B)** precursors. **(C)** The volcano plot of DEPs. **(D)** Principal component analysis (PCA) plots. (G1: Liver Cirrhosis Group; G2: HCC Group) **(E)** Heat map visualization of DEPs. (G1: Liver Cirrhosis Group; G2: HCC Group)

expression of DEPs differed considerably across the HCC and liver cirrhosis groups, as indicated in a heat map (Fig. 2E).

Analysis of functional enrichment of differentially abundant proteins

GO terms (Fig. 3A), KEGG pathways (Fig. 3B), and DO terms (Fig. 3C) with statistical differences in enrichment analysis hypergeometric tests were investigated in this study. Complement activation, humoral immune response mediated by circulating immunoglobulin, classical pathway of complement activation, plasma lipoprotein particle clearance, and positive regulation of lipid metabolic process were the top five annotation information of DEPs enriched in the biological process category of GO. Out of the top five annotation information of DEPs primarily enriched in the Cellular Component (CC) category of GO, 4 were related to lipoprotein particle. Complement and coagulation cascades was the top one annotation information of the DEPs primarily enriched in the KEGG

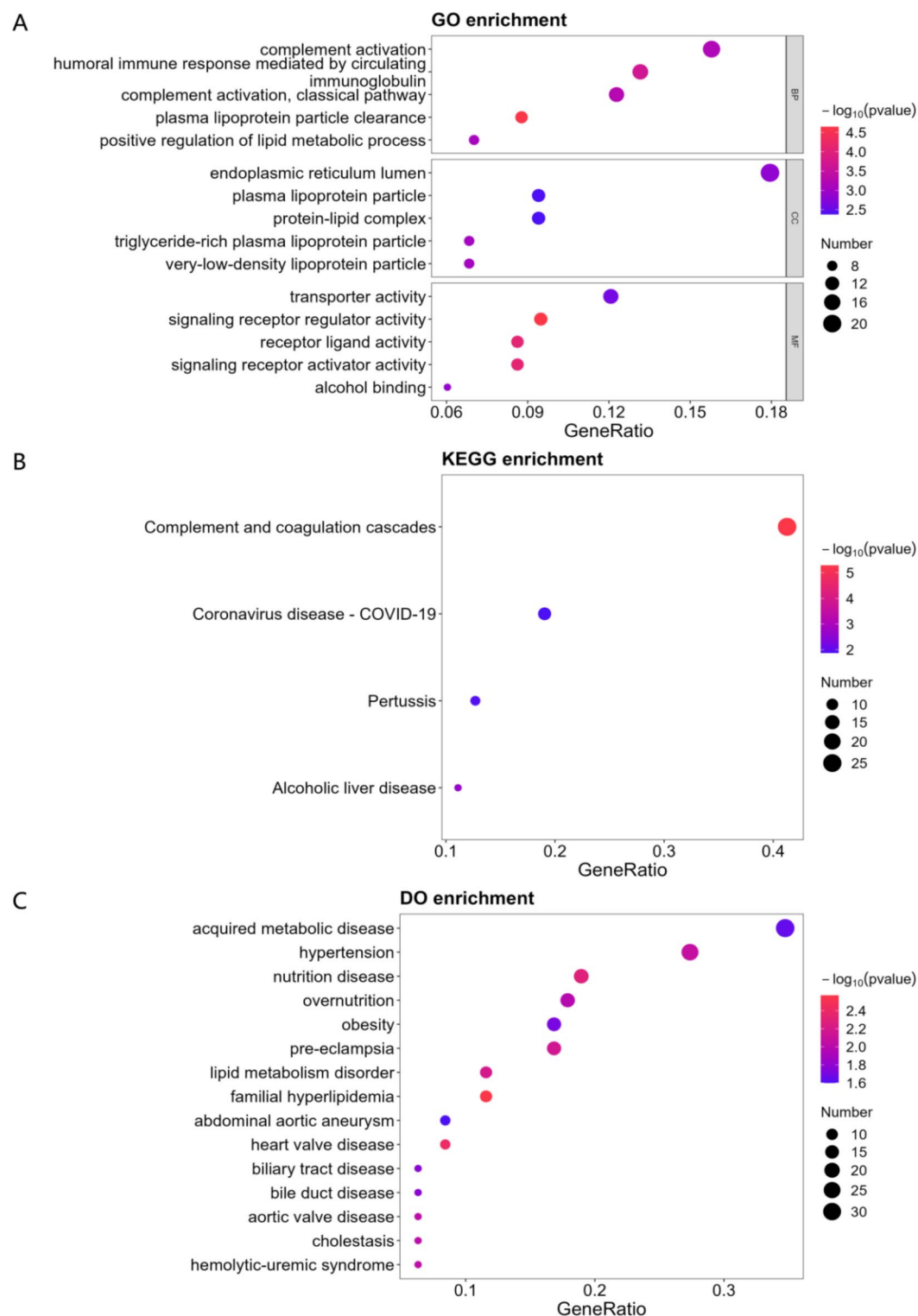


Fig. 3. Gene Ontology (GO), Kyoto Encyclopedia of Genes and Genomes (KEGG) and Disease Ontology (DO) analysis for 150 differentially expressed proteins (DEPs). (A) GO enrichment of DEPs ($p \leq 0.05$) displayed top 5 terms per category (ranked by p -value). (B) KEGG enrichment of DEPs ($p \leq 0.05$) showed the top 4 terms, ranked by p -value. (C) DO enrichment of DEPs ($p \leq 0.05$) showed the top 15 terms, ranked by p -value.

pathway. Out of the top fifteen annotation information of DEPs primarily enriched in the DO items, 40%(6/15) were related to lipid metabolism.

CytoScope software was used to establish network maps of DEPs with protein-protein interaction (PPI) data from the STRING database (Fig. 4A). In addition, using the “CytoHubba” plug-in, the hub proteins under four algorithms [DEGREE (Fig. 4B), Density of Maximum Neighborhood Component (DMNC) (Fig. 4C), Maximal Clique Centrality (MCC) (Fig. 4D) and Maximum Neighborhood Component (MNC) (Fig. 4E)] were further calculated. The hub proteins, which were selected from the top 10 proteins in each algorithm, were cross-analyzed

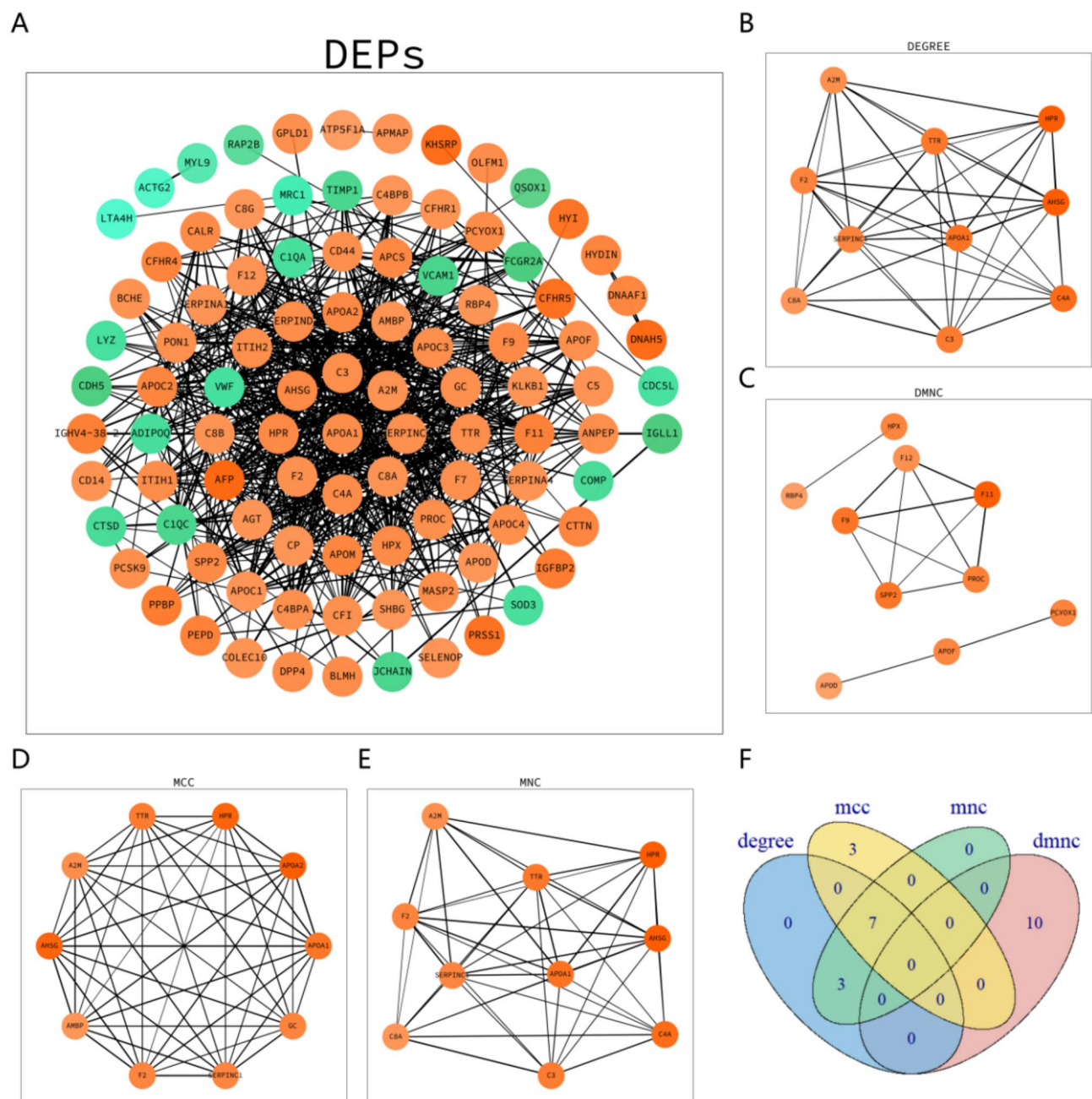
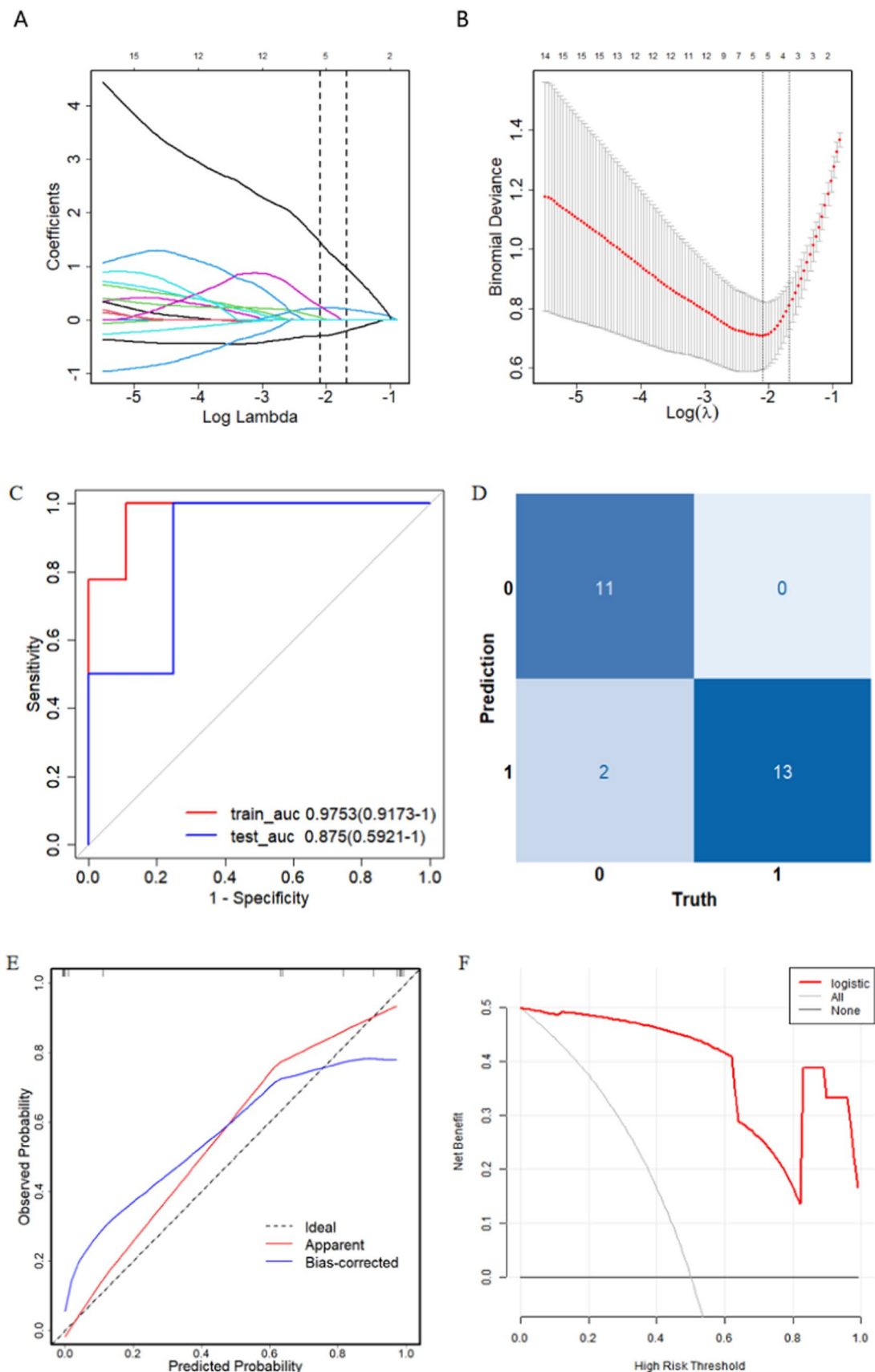


Fig. 4. Protein-protein interaction (PPI) network analysis of differentially expressed proteins (DEPs). **(A)** Network graph depicting the correlation of proteins derived from DEPs. **(B)** The hub proteins calculated under Degree Centrality (DEGREE). **(C)** The hub proteins calculated under Density of Maximum Neighborhood Component (DMNC). **(D)** The hub proteins calculated under Maximal Clique Centrality (MCC). **(E)** The hub proteins calculated under Maximum Neighborhood Component (MNC). **(F)** Venn diagram based on cross-analysis under four algorithms (DEGREE, DMNC, MCC and MNC). Circles indicated the gene symbol of protein, in which red and green indicated up-regulated and down-regulated proteins, respectively. The thickness of the lines represented the strength of the interaction. The darkness of the colors represented the magnitude of the discrepancy.



and mapped to Venn diagram (Fig. 4F). Apolipoprotein A-I (APOA1), TTR, Prothrombin (F2), Antithrombin-III (SERPINC1), Alpha-2-HS-glycoprotein (AHSG), Alpha-2-macroglobulin (A2M) and Haptoglobin-related protein (HPR) were finally identified as hub proteins (Fig. 4).

◀ **Fig. 5.** Differentially expressed proteins (DEPs) selection using Least Absolute Shrinkage and Selection Operator (LASSO) regression model, and the risk of HCC model evaluation. (A) LASSO coefficient profiles of the DEPs. (B) The relational graph between fitting error and $\log(\lambda)$. Dotted vertical lines were drawn at the optimal values by using the minimum criteria (min criteria) and the 1 standard error of the minimum criteria (1se criteria). λ value was chosen when the fitting error was minimum. (C) The receiver operating characteristic curve (ROC). (D) Confusion matrix. (E) Plot depicting the calibration. (F) Decision curve analysis curve. (G) Nomogram for predicting the risk of HCC. (H) Comparison of transthyretin levels in HCC and liver cirrhosis groups (27.45 ± 3.71 vs. 61.20 ± 3.64 mg/L, $t = 5.892$, $p < 0.001$). (I) Comparison of apolipoprotein A-1 levels in HCC and liver cirrhosis groups (2.41 ± 0.17 vs 1.75 ± 0.08 g/L, $t = 3.961$, $p < 0.001$).

Least absolute shrinkage and selection operator (LASSO) protein screening

The variables were filtered using LASSO regression. The penalty word was chosen using five-fold cross-validation. When the inaccuracy of the model was minimized, the parameter Lambda (λ) was employed (Fig. 5B), and 5 proteins were chosen for the future diagnostic model development (Fig. 5A). Figure 5A is a coefficient distribution diagram, with each line representing a protein and the end of each line pointing to a vertical coordinate reflecting the corresponding coefficients of each protein determined by LASSO. However, not all of these proteins are linked to disease, therefore the criteria in Fig. 5B must also function as thresholds to determine how many proteins can be employed for further investigation. The aforementioned parameter, which corresponds to the dotted line on the left side of Fig. 5B, is known as lambda.min. The value of lambda.min in Fig. 5B is 5, indicating that there are 5 protein coefficients that can be left. The 5 proteins screened out were immunoglobulin heavy variable 3–13 (IGHV3-13), far upstream element-binding protein 2, A2M, complement C5 and Xaa-Pro dipeptidase (Fig. 5A).

The creation of an HCC risk prediction model

Random combinations of the five selected DEPs were created, with the number of DEPs limited to 5, and five-cross-validation was performed based on the AUC value. Finally, the best DEP combination was chosen to build the clinical HCC prediction model, which included IGHV3-13 and A2M. The area under the ROC curve in Fig. 5C represents the capacity of the receiver operating characteristic curve to correctly discriminate patients with and without HCC. In Fig. 5C, a concordance index greater than 0.9 suggests that the model has a high degree of differentiation. Confusion matrix is shown in Fig. 5D. The sum of data in each row of the confusion matrix reflects the true number of the category, the sum of data in each column is the predicted number, and the value on the diagonal of the matrix represents the number of samples successfully predicted. The percentage of samples properly predicted by the model was 92.31% (24/26). Figure 5E is a calibration curve that depicts a scatter plot between the actual and predicted probability of occurrence. The calibration curve acquired through repeated Bootstrap self-sampling demonstrates that the trend trajectory of the simulated curve and the actual curve are essentially and strongly consistent. Figure 5F depicts a DCA decision curve. The black horizontal line and the blue diagonal line illustrate two extreme cases: the black horizontal line indicates that all samples are free of HCC, while the blue diagonal line indicates that all samples have HCC. In this study, the orange curve represents the actual fitting of the model. As shown in Fig. 5F, the orange curve outperforms the two extreme curves over a wide range, implying that this model can better differentiate patients with HCC. The Alignment Diagram in Fig. 5G consists mostly of the name of the left column and the corresponding line with a scale in the right column. A single fraction matching to IGHV3-13 and A2M under different values can be represented by a point in the figure. Total Point denotes the combined score of IGHV3-13 and A2M. The Risk value associated with the Total Point reflects the likelihood of having HCC.

Validation of APOA1 and TTR as plasma indicators of HCC in HIV/HBV co-infected patients

TTR and APOA1 levels were determined in 88 plasma samples from HIV/HBV co-infected people, 30 of whom had HCC and 58 of whom had liver cirrhosis. As shown in Fig. 5H, TTR levels in HIV/HBV co-infected patients with HCC and liver cirrhosis were significantly different, with plasma TTR levels of (27.45 ± 3.71) mg/L and (61.20 ± 3.64) mg/L, respectively ($t = 5.892$, $p < 0.001$). Similarly, in Fig. 5I, plasma APOA1 levels were (2.41 ± 0.17) g/L and (1.75 ± 0.08) g/L in patients with HCC and liver cirrhosis, respectively, showing that APOA1 levels differed significantly between the two groups ($t = 3.961$, $p < 0.001$).

Discussion

In China, HBV infection remains the predominant etiology of liver cirrhosis and HCC, with some cases progressing silently from cirrhosis to malignancy¹⁶. This progression is markedly accelerated in HIV/HBV co-infected individuals, who face a significantly elevated risk of HCC due to compounded liver injury. A critical clinical challenge lies in the early detection of HCC, as cirrhotic patients often remain asymptomatic until advanced stages, when therapeutic options are limited^{17,18}.

Proteomics has emerged as a powerful tool for unraveling disease mechanisms and identifying predictive biomarkers. Building on our previous work—where we developed a liver fibrosis prediction model for HIV/HBV co-infection¹⁹—this study extends the application of proteomic technology to address the continuum of liver disease progression: fibrosis, cirrhosis, and ultimately HCC. By systematically screening differentially expressed proteins (DEPs) in HIV/HBV co-infected patients with cirrhosis and HCC, we aim to identify early warning signatures of HCC onset. Such biomarkers could facilitate timely intervention, ultimately improving clinical outcomes for this high-risk population.

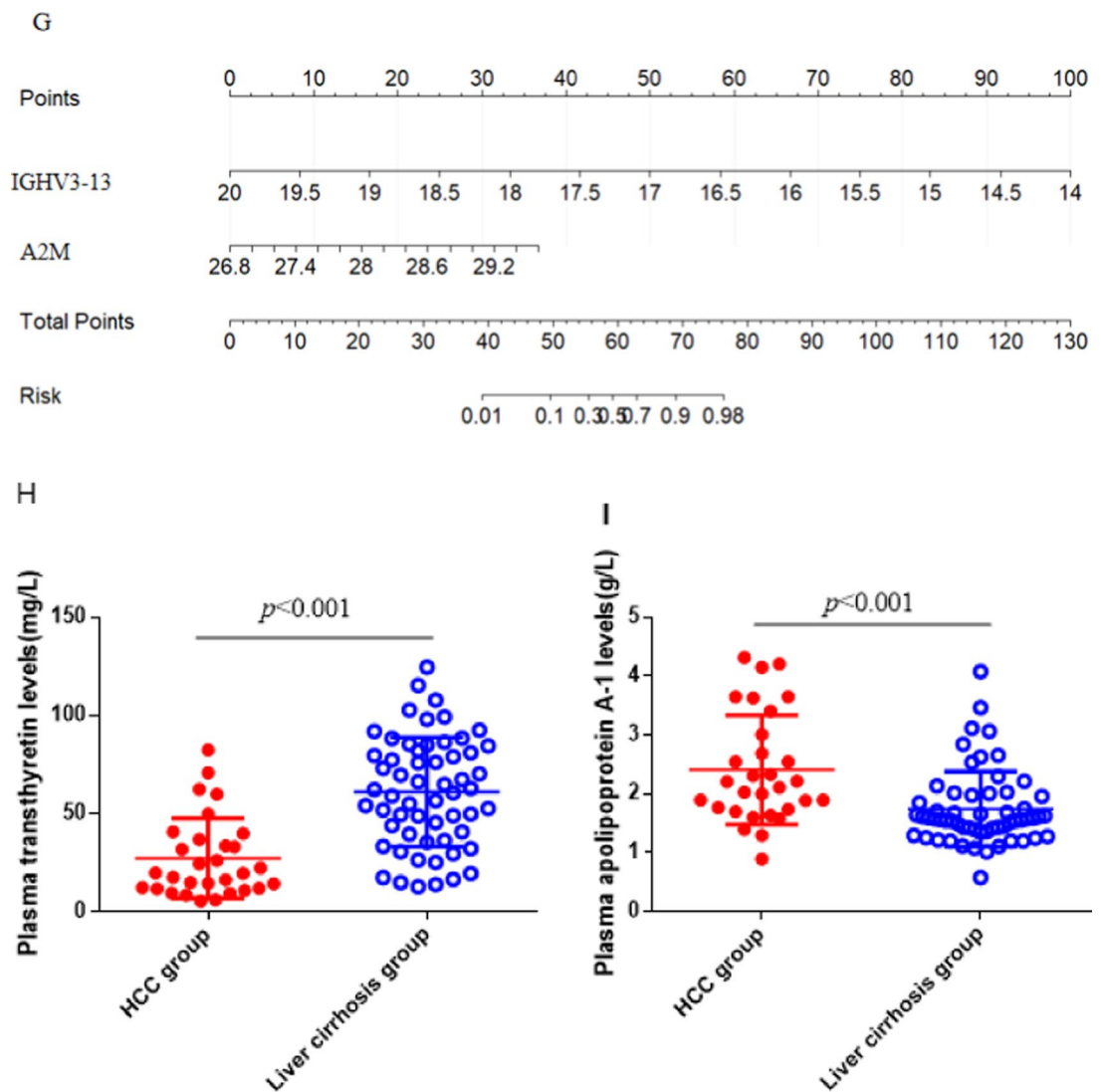


Figure 5. (continued)

The GO enrichment analysis revealed that DEPs were significantly enriched in lipoprotein metabolic processes, consistent with the observed upregulation of APOA-1 in HCC patients. As the major structural component of high-density lipoproteins, APOA-1 is primarily synthesized in the liver and small intestine and plays crucial roles in reverse cholesterol transport, platelet degranulation, and immune modulation. While numerous proteomic studies have proposed ApoA-1 as a potential tumor biomarker^{20–25}, its expression patterns in HCC remain controversial.

In the present study, we demonstrated elevated serum ApoA-1 levels in HCC patients compared to those with liver cirrhosis. This finding aligns with reports by Fye et al.²¹ and Pleguezuelo et al.²⁴, who identified increased APOA1 as an independent risk factor for HCC development. However, these observations contrast with other studies reporting decreased APOA1 levels in HCC^{22,25}. This apparent discrepancy may be explained by two competing mechanisms: First, HBV-induced liver dysfunction impairs hepatic APOA1 synthesis capacity, potentially through epigenetic silencing via CpG island hypermethylation²⁶. Second, emerging evidence suggests APOA1 may function as a tumor regulator, with studies demonstrating its ability to modulate cancer cell proliferation and metastasis²⁷. For instance, Kim et al.²⁸ reported that ginsenoside Rpl exerts antitumor effects through APOA1 upregulation, further supporting its potential role in tumor suppression. The observed ApoA-1 overexpression in HCC may represent a host defense mechanism through its potential role in malignant-to-normal cell transformation²⁹. This hypothesis gains support from clinical evidence demonstrating that HCC patients with lower ApoA-1 levels exhibit greater susceptibility to vascular invasion, as identified by mass spectrometry analyses³⁰. These findings suggest that ApoA-1 expression dynamics in HBV-related HCC are influenced by multiple factors, including hepatic functional reserve and systemic stress responses, which may account for the conflicting results across studies with heterogeneous patient populations at different disease stages.

Notably, emerging clinical evidence positions ApoA1 as a promising serological marker for early-stage HCC, with demonstrated utility in predicting tumor recurrence and patient survival³¹. This prognostic value has been formally incorporated into preoperative scoring systems for HCC management³². Beyond risk prediction, serial ApoA1 monitoring could enhance patient stratification and clinical decision-making, potentially improving HCC outcomes through earlier intervention and personalized treatment approaches.

Our proteomic analysis identified transthyretin (TTR, prealbumin) as another key differential protein between HBV-associated cirrhosis and HCC. As a hepatically synthesized protein, TTR serves as a sensitive indicator of liver synthetic function and correlates strongly with fibrosis severity. Clinical studies have established its prognostic value, particularly in patients with preserved liver function (Child-Pugh A), where TTR independently predicts post-hepatectomy survival^{33,34}. This evidence has led to the development of a modified Child-Pugh (MCP) scoring system incorporating TTR for more accurate liver function assessment. The potential diagnostic utility of TTR is supported by both experimental and clinical evidence. In diethylnitrosamine (DEN)-induced HCC models using male Wistar rats, TTR expression increased following hepatocarcinogenesis³⁵. This observation parallels clinical findings where elevated serum TTR levels demonstrate prognostic significance in HCC patients. Notably, validated predictive models incorporating TTR can effectively estimate 1-, 3-, and 5-year survival rates post-hepatectomy^{36,37}. Our findings further reinforce TTR's potential as a discriminative biomarker between cirrhosis and HCC, consistent with previous reports suggesting its utility in early HCC detection³⁸.

Our proteomic analysis of HBV-related liver cirrhosis and HCC patients revealed significant alterations in coagulation-related proteins, particularly fibrinogen (F2) and antithrombin III (ATIII/SERPINC1). These findings align with established knowledge that hepatic synthetic dysfunction in advanced liver disease markedly affects coagulation parameters. SERPINC1, identified through rigorous secretome-interactome-miRNA target analysis³⁹, has emerged as a particularly promising circulating biomarker for HCC detection. The clinical relevance of ATIII is underscored by multivariate analyses demonstrating that ATIII levels $\geq 70\%$ independently predict improved overall and disease-free survival post-hepatectomy⁴⁰.

Although some glycoprotein changes have been identified in the serum of patients with various liver diseases, providing potential glycan biomarkers for diagnosis, prognosis, and disease progression monitoring⁴¹, there are few reports on the relationship between a2-HS glycoprotein and HCC. Few studies using combined Kaplan–Meier models found that HCC stage III or IV with a content of AHSG (P02765) $< 0.2\%$ had the worst post-surgical recurrence-free and overall survival rates⁴². This study showed that a2-HS glycoprotein plasma expression in HCC patients is higher than in liver cirrhosis patients, which is a significant insight that warrants further investigation.

Because A2M is one of the acute phase proteins, a rise in A2M in HBV carriers may indicate active liver disease. In hypoalbuminemia, A2M levels may rise, possibly as a compensatory mechanism to maintain plasma colloid osmotic pressure. Furthermore, A2M is associated with platelet degranulation, humoral immune response, and negative modulation of immunological effector processes. Early research revealed that A2M was strongly connected to rat hepatocarcinogenesis and was found as a novel marker characteristic of rat hepatocellular preneoplastic and neoplastic lesions that was undetectable by well-established cytochemical markers⁴³. These findings, combined with our current results, suggest a potentially important yet complex relationship between A2M expression patterns and HCC progression that warrants systematic exploration in future studies.

Our study identified α -2-macroglobulin (A2M) as a significant biomarker in HBV-related liver disease progression. As an acute phase reactant, elevated A2M levels in HBV carriers may reflect active hepatic inflammation and disease activity. This elevation could represent a compensatory mechanism to maintain colloid osmotic pressure in hypoalbuminemic states, while simultaneously participating in platelet degranulation and immune response modulation. The oncogenic potential of A2M finds support in experimental hepatocarcinogenesis models, where it was identified as a specific marker for preneoplastic and neoplastic lesions in rat liver⁴⁴. Our clinical observations in human HCC parallel these experimental findings, demonstrating conserved pathophysiological mechanisms across species. Importantly, we established A2M's predictive value for HCC development in HBV-cirrhosis patients, though further studies are needed to determine precise diagnostic thresholds.

The potential involvement of haptoglobin-related protein (HPR) in hepatocellular carcinoma was first suggested by its detection in HepG2 cells nearly three decades ago⁴⁵, yet its clinical significance in HCC pathogenesis has remained unexplored until now. Our proteomic analysis identifies HPR as a novel differentially expressed protein in HBV-related cirrhosis and HCC, providing new avenues for understanding hepatocarcinogenesis mechanisms. Further characterization of HPR and other identified proteins may yield critical insights into HCC development pathways.

Of particular interest is our discovery of immunoglobulin heavy variable 3–13 (IGHV3–13) as a significantly dysregulated protein in HCC. While IGHV repertoire diversity and rearrangement are well-documented in hematologic malignancies^{46–48}, their role in solid tumors, particularly HCC, remains poorly understood. The selective expression of IGHV3–13 in HCC versus HBV-cirrhosis suggests a potential tumor-specific humoral immune response, which could inform both diagnostic strategies and immunotherapeutic development for HCC patients.

We acknowledge that there are some limitations with this study. First, as this HCC prediction model is based on a population of patients with HIV/HBV cirrhosis, the results' applicability to individuals with cirrhosis from other causes needs to be investigated further. This study did not include healthy persons as controls, therefore the predictive efficacy of HCC diagnostic model may be limited to clinical applications of patients with cirrhosis. Furthermore, the efficacy of combining the selected proteins with established HCC markers, such as AFP and aberrant F2, in the early detection of HCC has to be determined. Third, due to the restricted availability of current commercial kits, this study only confirmed ApoA1 and TTR, and additional validation investigations

on other core differentially expressed proteins should be performed when appropriate testing conditions are available. Lastly, AFP, a traditional marker of HCC, was not found in the DEPs of the proteomic analysis results in this study, which was related to the proportion of patients with liver cirrhosis who also had elevated AFP, the disease stage and surgical intervention of HCC patients in this study, and the small sample size. Future studies should take these parameters into account completely. Despite these limitations, the findings of this study will have a favorable influence, as they will contribute to a better understanding of the significance and role of differential protein in the early detection of HCC, in order to improve clinical diagnosis and treatment methods in the future.

Conclusions

The findings of this study demonstrated significant differences in the expression of 150 proteins between the liver cirrhosis group and the hepatocellular carcinoma (HCC) group, with 93 proteins up-regulated and 57 proteins down-regulated in the HCC group. Functional enrichment analysis revealed that these differentially expressed proteins were primarily associated with lipid metabolism, complement activation, and humoral immune response. Furthermore, seven core proteins-APOA1, SERPINC1, A2M, AHSG, F2, HPR, and TTR-were identified, and a risk assessment model for HCC in HIV/HBV co-infected patients with liver cirrhosis was successfully established.

These results underscore the critical importance of continued research into the molecular mechanisms underlying HCC development, particularly in high-risk populations such as HIV/HBV co-infected individuals. The identification of these core proteins and the development of the risk assessment model provide a practical framework for early detection and intervention, which could significantly improve clinical outcomes. Moreover, these findings offer valuable insights for the development of targeted therapeutic strategies, potentially leading to innovative treatments for HCC. This study highlights the translational potential of proteomic research in advancing personalized medicine and improving patient care in hepatology.

Data availability

The data presented in the study are deposited in the ProteomeXchange Consortium via the iProX repository, accession number PXD046369. IPX0007140002 in PXD046369 is the original sequence information of this study.

Received: 3 December 2024; Accepted: 16 April 2025

Published online: 07 May 2025

References

- Mao, X. et al. HBV-related HCC, cirrhosis, and HBsAg seroclearance: A systematic review and meta-analysis. *Hepatology* **77** (5), 1735–1745 (2023). Steatosis.
- Wang, H. et al. Hepatitis B infection in the general population of China: A systematic review and meta-analysis. *BMC Infect. Dis.* **19** (1), 811 (2019).
- Yang, R. et al. Long-term observation on hepatitis B surface antigen seroclearance in therapy experienced HIV/HBV co-infected Chinese. *J. Viral Hepat.* **27** (2), 127–134 (2020).
- Leumi, S. et al. Global burden of hepatitis B infection in people living with human immunodeficiency virus: A systematic review and Meta-analysis. *Clin. Infect. Dis.* **71** (11), 2799–2806 (2020).
- Robbins, H. A. et al. Epidemiologic contributions to recent cancer trends among HIV-infected people in the United States. *AIDS* **28**(6):881–890. (2014).
- Vullierme, M. P. et al. Hepatocellular carcinoma—what's new? *J. Visc. Surg.* **147** (1), e1–12 (2010).
- Chen, S. et al. Differential expression of plasma microRNA-125b in hepatitis B virus-related liver diseases and diagnostic potential for hepatitis B virus-induced hepatocellular carcinoma. *Hepatol. Res.* **47** (4), 312–320 (2017).
- Luo, P. et al. Current status and perspective biomarkers in AFP negative HCC: Towards screening for and diagnosing hepatocellular carcinoma at an earlier stage. *Pathol. Oncol. Res.* **26** (2), 599–603 (2020).
- Bruix, J. & Sherman, M. American association for the study of liver diseases. Management of hepatocellular carcinoma: an update. *Hepatology* **53** (3), 1020–1022 (2011).
- Xun, Z. et al. Proteomic characterization of the natural history of chronic HBV infection revealed by tandem mass tag-based quantitative proteomics approach. *Mater. Today Bio.* **15**, 100302 (2022).
- Gao, Q. et al. Integrated proteogenomic characterization of HBV-Related hepatocellular carcinoma. *Cell* **179** (2), 561–577e22 (2019).
- Geyer, P. E. et al. Revisiting biomarker discovery by plasma proteomics. *Mol. Syst. Biol.* **13** (9), 942 (2017).
- Huang, H. et al. Serum metabolomic signatures discriminate early liver inflammation and fibrosis stages in patients with chronic hepatitis B. *Sci. Rep.* **6**, 30853 (2016).
- Sousa, M. M., Berglund, L. & Saraiva, M. J. Transthyretin in high density lipoproteins: Association with Apolipoprotein A-I. *J. Lipid Res.* **41** (1), 58–65 (2000).
- Siddiqui, K. et al. Cholesterol pathway biomarkers are associated with neuropsychological measures in multiple sclerosis. *Mult. Scler. Relat. Disord.* **69**, 104374 (2023).
- Takano, S. et al. Incidence of hepatocellular carcinoma in chronic hepatitis B and C: A prospective study of 251 patients. *Hepatology* **21** (3), 650–655 (1995).
- Bruix, J., Reig, M. & Sherman, M. Evidence-Based diagnosis, staging, and treatment of patients with hepatocellular carcinoma. *Gastroenterology* **150** (4), 835–853 (2016).
- Obi, S. et al. Combination therapy of intraarterial 5-fluorouracil and systemic interferon-alpha for advanced hepatocellular carcinoma with portal venous invasion. *Cancer* **106** (9), 1990–1997 (2006).
- Yuan, R. et al. A novel plasma proteomic-based model for predicting liver fibrosis in HIV/HBV co-infected adults. *J. Med. Virol.* **95**(1):e28222. (2023).
- Zamanian-Daryoush, M. & DiDonato, J. A. Apolipoprotein A-I and cancer. *Front. Pharmacol.* **6**, 265 (2015).
- Fye, H. K. et al. Protein profiling in hepatocellular carcinoma by label-free quantitative proteomics in two West African populations. *PLoS One.* **8** (7), e68381 (2013).
- Gao, H. J. et al. Quantitative proteomic analysis for high-throughput screening of differential glycoproteins in hepatocellular carcinoma serum. *Cancer Biol. Med.* **12** (3), 246–254 (2015).

23. Dillon, S. T. et al. Quantitative proteomic analysis in HCV-induced HCC reveals sets of proteins with potential significance for racial disparity. *J. Transl Med.* **11**, 239 (2013).
24. Pleguezuelo, M. et al. Proteomic analysis for developing new biomarkers of hepatocellular carcinoma. *World J. Hepatol.* **2** (3), 127–135 (2010).
25. Mustafa, M. G. et al. Biomarker discovery for early detection of hepatocellular carcinoma in hepatitis C-infected patients. *Mol. Cell. Proteom.* **12** (12), 3640–3652 (2013).
26. Wang, Y. et al. The mechanism of apolipoprotein A1 down-regulated by hepatitis B virus. *Lipids Health Dis.* **15**, 64 (2016).
27. Zamanian-Daryoush, M. et al. The cardioprotective protein Apolipoprotein A1 promotes potent anti-tumorigenic effects. *J. Biol. Chem.* **288** (29), 21237–21252 (2013).
28. Kim, M. Y., Yoo, B. C. & Cho, J. Y. Ginsenoside-Rp1-induced Apolipoprotein A-1 expression in the LoVo human colon cancer cell line. *J. Ginseng Res.* **38** (4), 251–255 (2014).
29. Ma, X. L. et al. Apolipoprotein A1: A novel serum biomarker for predicting the prognosis of hepatocellular carcinoma after curative resection. *Oncotarget* **7** (43), 70654–70668 (2016).
30. Xu, X. et al. Identification of two portal vein tumor thrombosis associated proteins in hepatocellular carcinoma: Protein disulfide-isomerase A6 and Apolipoprotein A-I. *J. Gastroenterol. Hepatol.* **26** (12), 1787–1794 (2011).
31. Ni, X. C. et al. Role of lipids and apolipoproteins in predicting the prognosis of hepatocellular carcinoma after resection. *Onco Targets Ther.* **13**, 12867–12880 (2020).
32. Mao, M. et al. A novel score based on serum Apolipoprotein A-1 and C-reactive protein is a prognostic biomarker in hepatocellular carcinoma patients. *BMC Cancer.* **18** (1), 1178 (2018).
33. Wen, X. et al. Integration of prealbumin into Child–Pugh classification improves prognosis predicting accuracy in HCC patients considering curative surgery. *J. Clin. Transl Hepatol.* **6** (4), 377–384 (2018).
34. Fan, Y. et al. Preoperative serum prealbumin level and adverse prognosis in patients with hepatocellular carcinoma after hepatectomy: A meta-analysis. *Front. Oncol.* **11**, 775425 (2021).
35. Katare, P., Malik, D. & Mani, S. J. Novel mutations in transthyretin gene associated with hepatocellular carcinoma. *Mol. Carcinog.* **57** (1), 70–77 (2018).
36. Shimura, T. et al. Clinical significance of serum transthyretin level in patients with hepatocellular carcinoma. *ANZ J. Surg.* **88** (12), 1328–1332 (2018).
37. Huo, R. R. et al. Development and validation of a nomogram for assessing survival in patients with hepatocellular carcinoma after hepatectomy. *Biosci. Rep.* **40** (6), BSR20192690 (2020).
38. Huang, H. et al. Identification of the level of exosomal protein by parallel reaction monitoring technology in HCC patients. *Int. J. Gen. Med.* **15**, 7831–7842 (2022).
39. Awan, F. M. et al. Identification of Circulating biomarker candidates for hepatocellular carcinoma (HCC): An integrated prioritization approach. *PLoS One.* **10** (9), e0138913 (2015).
40. Iwako, H. et al. Prognostic significance of antithrombin III levels for outcomes in patients with hepatocellular carcinoma after curative hepatectomy. *Ann. Surg. Oncol.* **19** (9), 2888–2896 (2012).
41. Cao, X. et al. Combination of serum Paraoxonase/arylesterase 1 and antithrombin-III is a promising non-invasion biomarker for discrimination of AFP-negative HCC versus liver cirrhosis patients. *Clin. Res. Hepatol. Gastroenterol.* **45** (5), 101583 (2021).
42. Inoue, T. & Tanaka, Y. Novel biomarkers for the management of chronic hepatitis B. *Clin. Mol. Hepatol.* **26** (3), 261–279 (2020).
43. Chang, T. T. & Ho, C. H. Plasma proteome atlas for differentiating tumor stage and post-surgical prognosis of hepatocellular carcinoma and cholangiocarcinoma. *PLoS One.* **15** (8), e0238251 (2020).
44. Sukata, T. et al. alpha(2)-Macroglobulin: A novel cytochemical marker characterizing preneoplastic and neoplastic rat liver lesions negative for hitherto established cytochemical markers. *Am. J. Pathol.* **165** (5), 1479–1488 (2004).
45. Tabak, S. et al. Transcriptionally active haptoglobin-related (Hpr) gene in hepatoma G2 and leukemia molt-4 cells. *DNA Cell Biol.* **15** (11), 1001–1007 (1996).
46. Thörnqvist, L. & Ohlin, M. The functional 3'-end of Immunoglobulin heavy chain variable (IGHV) genes. *Mol. Immunol.* **96**, 61–68 (2018).
47. Katsibardi, K. et al. Clinical significance of productive Immunoglobulin heavy chain gene rearrangements in childhood acute lymphoblastic leukemia. *Leuk. Lymphoma.* **52** (9), 1751–1757 (2011).
48. Marti, G. E. et al. Long-term follow-up of monoclonal B-cell lymphocytosis detected in environmental health studies. *Cytometry B Clin. Cytom.* **78** (Suppl 1), S83–90 (2010).

Acknowledgements

We thank the patients, the nurses and physicians who provided care for the patients, and the investigators at Zhongnan Hospital of Wuhan University. We thank SpecAlly Life Technology Co, Ltd, Wuhan, China for providing technical support.

Author contributions

RR.Y., YX.Z. and Hengning Ke conceived of and designed the study. Xingxia Yu and Rui Yuan collected and analyzed the data. Hui Hu and Wenjia Hu collected samples. Ke Zhuang, Mingqi Luo and Yong Yang performed the experiments. Yong Yang, Hengning Ke, Xien Gui and Rongrong Yang provided suggestions. All authors contributed to the study and approved the submitted version.

Funding

This study was supported by National Natural Science Foundation of China (Grant No. 82003511), Discipline and Platform Construction Project of Center for AIDS Research, Wuhan University (PTPP2023002).

Declarations

Competing interests

The authors declare no competing interests.

Ethics approval

This study was approved by the Ethics Committee of Zhongnan Hospital of Wuhan University, and all individuals signed an informed consent form.

Additional information

Correspondence and requests for materials should be addressed to R.Y.

Reprints and permissions information is available at www.nature.com/reprints.

Publisher's note Springer Nature remains neutral with regard to jurisdictional claims in published maps and institutional affiliations.

Open Access This article is licensed under a Creative Commons Attribution-NonCommercial-NoDerivatives 4.0 International License, which permits any non-commercial use, sharing, distribution and reproduction in any medium or format, as long as you give appropriate credit to the original author(s) and the source, provide a link to the Creative Commons licence, and indicate if you modified the licensed material. You do not have permission under this licence to share adapted material derived from this article or parts of it. The images or other third party material in this article are included in the article's Creative Commons licence, unless indicated otherwise in a credit line to the material. If material is not included in the article's Creative Commons licence and your intended use is not permitted by statutory regulation or exceeds the permitted use, you will need to obtain permission directly from the copyright holder. To view a copy of this licence, visit <http://creativecommons.org/licenses/by-nc-nd/4.0/>.

© The Author(s) 2025